Biosafety and Health 6 (2024) 178–185

Contents lists available at ScienceDirect

Biosafety and Health

journal homepage: www.elsevier.com/locate/bsheal

Original Research

A novel method to assess antibody-dependent cell-mediated cytotoxicity against influenza A virus M2 in immunized murine models

Yinjie Liang [a,b], Junjia Guo [b,c], Zhen Li [a,b], Shiyuan Liu [b,d], Ting Zhang [a], Shucai Sun [b,e], Funa Lu [b,f], Yuqian Zhai [b], Wenling Wang [b,*], Chuanyi Ning [a,*], Wenjie Tan [b,c,*,1]

[a] Collaborative Innovation Centre of Regenerative Medicine and Medical BioResource Development and Application Co-constructed by the Province and Ministry, Guangxi Medical University, Nanning 530021, China
[b] Key Laboratory of Biosafety, National Health Commission of the People's Republic of China, National Institute for Viral Disease Control and Prevention, Chinese Center for Disease Control and Prevention, Beijing 102206, China
[c] School of Laboratory Medicine, Wenzhou Medical University, Wenzhou 325035, China
[d] School of Public Health, Baotou Medical College, Baotou 014040, China
[e] Department of Nuclear Medicine, The Second Hospital of Hebei Medical University, Shijiazhuang 050000, China
[f] Department of Microbiology, School of Basic Medicine, Inner Mongolia Medical University, Hohhot 010110, China

ARTICLE INFO

Article history:
Received 4 March 2024
Revised 13 April 2024
Accepted 16 April 2024
Available online 17 April 2024

Keywords:
Antibody-dependent cell-mediated cytotoxicity (ADCC)
Influenza A virus (IAV)
Matrix protein 2 extracellular domain (M2e)
Cell line

ABSTRACT

The matrix protein 2 (M2) is a preferred target for developing a universal vaccine against the influenza A virus (IAV). This study aimed to develop a method for assessing antibody-dependent cell-mediated cytotoxicity (ADCC) associated with M2-based immunization in mice. We first established a stable cell line derived from mouse lymphoma cells (YAC-1) expressing M2 of H3N2. This cell line, designated as YAC-1-M2, was generated using a second-generation lentiviral tricistronic plasmid system to transduce the *M2* gene into YAC-1 cells. The ADCC effect induced by polyclonal antibodies targeting matrix protein 2 ectodomain (M2e) was demonstrated by YAC-1-M2 cell lysis by natural killer cells (NK) derived from mice, in the presence of anti-M2 antibodies obtained from mice immunized with an mRNA vaccine based on M2e. This ADCC effect was found to be stronger compared to the effect induced by monoclonal antibodies (14C2) against M2. Moreover, the ADCC effect was enhanced as the effector-to-target ratio of NK to YAC-1-M2 cells increased. In conclusion, we established a novel method to detect ADCC of M2 of IAV, which paves the way for the development of an M2-based universal vaccine against IAV and an in-depth analysis of its mechanism of broad-spectrum immune protection in mice.

1. Introduction

The matrix-2 (M2) protein of influenza A virus (IAV) is a non-glycosylated protein present on the virus surface and consists of three distinct regions: extracellular domain (M2e), transmembrane domain, and intracellular domain [1]. M2 exhibits proton-selective channel activity and plays a crucial role in maintaining pH balance within the cytoplasm and Golgi apparatus. This facilitates viral entry into the host cells and contributes to the maturation and assembly of the virus, followed by replication and amplification within the host cell [2,3]. The sequence of the M2e domain is highly conserved and consists of 23 amino acids [4]. Despite lacking neutralizing activity [5], serum or monoclonal antibodies generated by M2/M2e immunization show significant protective effects when passively transferred to animals [6–9], and can lead to the elimination of virus-infected cells through antibody-dependent cell-mediated cytotoxicity (ADCC) [10].

The process of ADCC unfolds in several steps. Initially, the Fab region of the antibody recognizes the target cell, leading to cross-linking of the antibody's Fc segment with its receptor FcR expressed on the surface of effector cells. Ultimately, the Fc-FcR interaction triggers cytotoxic effects resulting in target cell destruction [11]. Several cell types in the peripheral blood express Fc receptors (FcRs) associated with the triggering of ADCC. Natural killer (NK) cells characterized by a high expression of FcγRIIIa (CD16) are the optimal mediators of ADCC [11]. Currently, the various established methods for detecting ADCC are typically categorized into two types: those

* Corresponding authors: Key Laboratory of Biosafety, National Health Commission of the People's Republic of China, National Institute for Viral Disease Control and Prevention, Chinese Center for Disease Control and Prevention, Beijing 102206, China (W. Wang and W. Tan); Collaborative Innovation Centre of Regenerative Medicine and Medical BioResource Development and Application Co-constructed by the Province and Ministry, Guangxi Medical University, Nanning 530021, China (C. Ning).

E-mail addresses: wangwl@ivdc.chinacdc.cn (W. Wang), ningchuanyi@126.com (C. Ning), tanwj@ivdc.chinacdc.cn (W. Tan).

[1] Given his role as Editorial Board Member, Wenjie Tan had no involvement in the peer-review of this article and had no access to information regarding its peer-review. Full responsibility for the editorial process for this article was delegated to Editor Di Qu.

https://doi.org/10.1016/j.bsheal.2024.04.002
2590-0536/

HIGHLIGHTS

Scientific question

Low expression of matrix protein 2 (M2) in cells infected with the influenza virus hampers studies.

Evidence before this study

The protective role of influenza virus M2 through antibody-dependent cell-mediated cytotoxicity (ADCC) is demonstrated. Inducing ADCC can effectively clear virus-infected cells, serving as a vital bridge between humoral and cellular immunity, as previous studies have suggested. Therefore, the selection of candidate vaccines capable of eliciting both broad neutralizing antibodies and potent ADCC is crucial for controlling influenza A virus outbreaks.

New findings

A stable cell line (YAC-1-M2) capable of sustaining M2 expression was established. The optimal effector-to-target cell ratio for this target cell is 20:1, and the IgG2a subtype is more effective in inducing ADCC compared to the IgG1 subtype.

Significance of the study

This study facilitates comprehension of the immunoprotective mechanisms associated with M2 and lays the groundwork for the development of vaccines and drugs based on non-neutralizing antibody protection mechanisms.

based on target cells and those based on effector cells. The methods based on target cells are the chromium release assay [12], flow cytometry using dye-labeled cells [13–15], and lactate dehydrogenase (LDH) release assay [16]. The most advanced methods for detecting ADCC based on effector cells are esterase release [17], perforin deposition [18], and CD107a degranulation [19] assays.

Most research on ADCC detection methods involves influenza virus hemagglutinin (HA), with only a few studies associated with the M2 protein. No applicable and convenient method is available to assess ADCC associated with M2-based immunization in mice, which is likely attributable to the low expression of M2 in cells infected with the influenza virus. Additionally, a significant challenge arises from the limited availability of target cells that can efficiently express influenza virus M2 at scale. To address these challenges, the study constructed a stable expression system for the IAV M2 protein using a lentiviral vector (pLV3-CMV-M2-FLUC, psPAX2, and pMD2). YAC-1 cells (a murine lymphoma cell line) were engineered as target cells to assess ADCC of influenza virus M2. Mouse NK cells served as effector cells and ADCC efficacy was evaluated using monoclonal and polyclonal antibodies against the M2 ectodomain. This platform is expected to provide a viable approach to investigate the immune-protective mechanisms induced by M2.

2. Materials and methods

2.1. Cloning of the M2 gene sequence

The IAV *M2* gene sequence was obtained from influenza virus A3/Beijing/30/95 (H3N2) [20] and optimized using mammalian codons. The Gluc2 signaling peptide was introduced [21]. The T2A sequence was used to link the downstream *M2* gene to the Firefly Luciferase gene (*F-Luc*) (GenBank: M15077.1), resulting in Gluc2-M2-T2a-Fluc. *Eco*RI restriction sites were introduced at both ends of the sequence to facilitate subsequent gene cloning. The gene sequence was synthesized using GenScript, and the gene fragment was inserted into the eukaryotic expression vector pcDNA3.1 to construct the recombinant plasmid pcDNA3.1-M2-FLUC.

2.2. Construction of a lentiviral vector containing the M2 gene

The Gluc2-M2-T2a-Fluc fragment from *Eco*RI-cleaved pcDNA3.1-M2-FLUC plasmid was inserted into *Eco*RI-linearized pLV3-CMV-MCS-3 × FLAG-CopGFP-Puro vector plasmid (Miaoling Biology, Wuhan, China) by ligation. The resulting ligation product was transformed into DH5α competent bacteria that were subsequently cultured overnight on LB agar plates supplemented with ampicillin (100 mg/mL) at 37 ˚C. Positive clones were identified by colony polymerase chain reaction (PCR) and selected for plasmid extraction, enzyme digestion, and sequencing confirmation. The resulting plasmid was designated pLV3-CMV-M2-T2A-FLUC-3 × FLAG-CopGFP-Puro (pLV3-M2-FLUC).

2.3. Lentivirus packaging and titer determination

A second-generation lentiviral tricistronic plasmid system comprising pLV3-M2-FLUC, psPAX2, and pMD2 was used for lentivirus packaging. Plasmid pLV3-M2-FLUC contains the target gene *M2*, human Immunodeficiency virus (HIV) core elements 5′ long terminal repeat (LTR) and 3′ LTR, and accessory elements such as the HIV envelope protein, gp41. Plasmid psPAX2 harbors coding sequences for the major HIV viral protein Gag and the polymerase Pol. Additionally, plasmid pMD2.G carries the envelope gene, *VSV-G*. The three plasmids (pLVX, pSPAX2, and pMD2.G) were transfected in a ratio of 4:3:1 (1.00 μg : 0.75 μg : 0.25 μg) and mixed with transfection reagent HP (Roche) in a ratio of 50 μL : 150 μL. After thorough mixing, the mixture was incubated at room temperature for 15 min and added dropwise to 293 T cells at 80 % confluency. The cells were gently shaken, placed in a 37 ˚C incubator, and observed under an inverted fluorescence microscope for *CopGFP* (Copepoda green fluorescent protein) expression. Cell culture supernatants were collected after 48 h. After centrifugation to remove cell debris, the supernatant was concentrated using a lentivirus concentration kit (Bomeid). This process yielded lentiviruses expressing the M2 protein (Lentivirus-M2, LV-M2). The viral titer of LV-M2 cells was determined using an infectious titer assay [22]. The lentiviral titer was calculated based on the CopGFP expression rate as follows: lentiviral titer (IU/mL) = seeded cell count × infected cell percentage (%) / inoculated virus volume.

2.4. Screening and identification of stable M2-FLUC cell lines

YAC-1 cells were inoculated into a 48-well plate and varying puromycin concentrations (0.0, 0.5, 1.0, 1.5, 2.0, 2.5, 3.0, 3.5, 4.0, 4.5, and 5.0 μg/mL; Thermo Fisher Scientific, USA) were added to individual wells. Cell viability and counts were determined daily under a microscope. The minimum puromycin concentration resulting in complete cell death was determined as the selective pressure screening concentration. YAC-1 cells were infected with lentivirus LV-M2. The fresh selection medium was replenished every three days, and the proportion of viable cells was monitored daily. LV-M2-infected cells exhibiting strong green fluorescence were isolated using flow cytometry to obtain monoclonal cell lines. FLUC activity was assessed following the expansion of the culture. YAC-1-M2 cells were seeded at a density of 1×10^4 cells/200 μL per well in a 96-well plate, with three parallel wells. After overnight incubation, D-lucifer in potassium salt (100 μL) was added to each well, followed by incubation at 37 ˚C for 10 min. Fluorescence values were determined using a multifunctional microplate reader to quantify relative FLUC expression. The cell lines with high FLUC expression were selected for further expansion and cultivation.

2.5. Quantitative real-time polymerase chain reaction (RT-qPCR)

Primers for the *M2* gene and the internal reference gene β-actin were designed using Primer Premier 5.0 software and synthesized by Qingke Biology Co., Ltd. The primers for *M2* were M2-F: 5′-GTCTCT GCTGACCGAGGTG-3′ and M2-R: 5′-AAACTCTCAGTGGTGGTGGTG-3′ , while those for β-actin were F: 5′-CATGTACGTTGCTATCCAGGC-3′ and R: 5′-CTCCTTAATGTCACGCACGAT-3′. The mRNA was extracted from 15th-generation YAC-1-M2 cells using a nucleic acid extraction kit (Tianlong Science and Technology Co., Ltd., China) and subjected to one-step qRT-PCR using SYBR Green PCR kit (Novozymes). The amplification conditions were as follows: reverse transcription at 50 ˚C for 3 min, denaturation at 95 ˚C for 30 s, followed by 40 cycles of 95 ˚C for 10 s and 60 ˚C for 30 s, with melting curve analysis at 95 ˚C for 15 s, 60 ˚C for 60 s, and 95 ˚C for 15 s.

2.6. Western blotting

The cell lysate was prepared by thoroughly mixing 1 mL of RIPA (CellSolab) with 10 μL of protease inhibitor (phenylmethylsulphonyl fluoride (PMSF), Solab). YAC-1-M2 cells were seeded in a 6-well plate at a density of 1×10^6 cells per well in 2 mL of medium and cultured overnight until 70 % – 80 % confluency. Thereafter, the cells were centrifuged, the supernatant was discarded, and 250 μL of lysis buffer was added to the cell pellet in each well. The samples were subjected to ice bath lysis for 10 min, followed by centrifugation at 12,000 *g* for 5 min at 4 ˚C. The supernatant was aspirated, and 10 μL of 6 × sample loading buffer was added. After thorough mixing, the samples were boiled for 10 min and subjected to sodium dodecyl sulfate polyacrylamide gel electrophoresis (80 V for 25 min, followed by 120 V for 1 h). Following electrophoresis, the proteins were transferred onto a polyvinylidene fluoride membrane (Pall Company) and blocked with 5 % skim milk at 25 ˚C for 2 h. The membrane was incubated overnight at 4 ˚C with a 1:1,000 dilution of the influenza virus M2 monoclonal antibody, 14C2 (Abcam). After washing, the membrane was incubated at room temperature for 1 h with a 1:5,000 dilution of goat anti-mouse IgG DyLight 800 (Sigma-Aldrich). Protein bands were detected using an Amersham ImageQuant 800 western blot imaging system.

2.7. Immunofluorescence assay

YAC-1-M2 monoclonal cells were seeded in 24-well plates. At approximately 80 % confluency, the cells were fixed with 4 % paraformaldehyde for 30 min. The expression of M2 protein in stable cell lines was detected using an indirect immunofluorescence assay with 14C2 as the primary antibody and a fluorescently labeled goat anti-mouse IgG (H + L) as the secondary antibody (Alexa Fluor™ Plus 594, Thermo Fisher Scientific).

2.8. Isolation and purification of mouse NK cells

Six to eight-week-old specific pathogen-free female BALB/c mice (Charles River Laboratories) were used under aseptic conditions for spleen extraction. The spleens were minced and the resulting homogenate was transferred to a centrifuge tube. An equal volume of the NK cell separation solution was gently added along the tube wall using a pipette. Centrifugation was subsequently performed at 206 *g* for 30 min to allow for liquid stratification. The intermediate cloudy white layer was carefully aspirated using a pipette. NK cells were isolated by negative selection using an NK cell isolation kit (Miltenyi Biotec, Germany). This involved labeling non-NK cells in a cell suspension with a mixture of biotin-conjugated antibodies and anti-biotin microbeads. The cell suspension was passed through a magnetic column, and the flow-through containing the purified NK cells was collected. High-purity unmarked NK cells were isolated by marking and removing non-target cells. To identify NK cells, the cell population was resuspended in 200 μL of 2 % fetal bovine serum (FBS) in phosphate-buffered saline (PBS). Subsequently, 5 μL of fluorescein isothiocyanate (FITC) Rat Anti-Mouse CD49b and 2 μL of allophycocyanin (APC) Hamster Anti-Mouse CD3e (both obtained from BD Biosciences) were added to the suspension. Cells positive for CD3e and CD49b (denoted as $CD3e^{-}CD49b^{+}$) were considered as NK cells.

2.9. Antibody detection and immunoprotective effect

Forty female BALB/c mice, aged 6–8 weeks, were randomly divided into two groups (n = 20 each) and immunized with 30 μg of lipopolyplex (LPP)-4M2eNP or LPP (negative control) via intramuscular injection. The initial immunization was followed by a booster shot after a 4-week interval, completing a total of two immunizations. Five mice from each group were sampled two weeks after each immunization for fluid immune response assessment using enzyme-linked immunosorbent assay (ELISA)[23]. Subsequently, two weeks after the final immunization, the mice were challenged with PR8 (H1N1) virus (20 × Lethal Dose 50 [LD_{50}]) (10 mice per group). Continuous observation for 14 days included recording changes in mouse body weight and monitoring mortality.

2.10. IAV M2 ADCC assay

Isolated and purified NK cells were cultured in Roswell Park Memorial Institute (RPMI) 1640 medium containing 10 % FBS and stimulated overnight with 200 U/mL Interleukin 2 (IL-2). The YAC-1-M2 cells were seeded at a density of 1×10^4 cells per well in 96-well plates. The NK cells (effector cells) were subsequently added to the YAC-1-M2 culture wells at 20:1, 10:1, and 5:1 ratios of NK cells to target cells. Each well was supplemented with monoclonal antibody M2 (14C2) against IAV M2 or mouse serum (obtained from mice immunized with 30 μg of LPP-4M2eNP mRNA vaccine in two doses, prepared by our laboratory, unpublished). Concurrently, wells were set up with NK + YAC-1-M2 cells without antibodies, together with wells with YAC-1-M2 cells alone. The cells were placed in a 37 ˚C, 5 % CO_2 humidified incubator for 16 h. ADCC was assessed using the LDH-Glo Cytotoxicity Assay Kit (Promega, Madison, WI, USA) according to the manufacturer's instructions. YAC-1-M2 wells were treated with 4 μL of 10 % Triton X-100 and incubated for 15 min to lyse the cells as the maximum release control wells. NK + YAC-1-M2 and YAC-1 cells were used as spontaneous-release control wells. Following centrifugation of cell samples from the experimental wells NK + Ab + YAC-1-M2 and others, 5 μL of supernatant was collected and diluted with 1 mL of LDH buffer (200 mol/L Tris-HCl, 10 % glycerol, and 1 % bovine serum albumin in PBS). Subsequently, 50 μL of the diluted samples were reacted at room temperature with an equal volume of LDH detection reagent for 45 min, and chemiluminescence intensity was measured using a multifunctional enzyme-linked immunosorbent assay reader. The cell killing rate was calculated according to the following formula [24]:

$$\text{Cell killing rate (\%)} = (LDH_{\text{experimental group release}} - LDH_{\text{effector cell spontaneous release}} - LDH_{\text{target cell spontaneous release}}) / (LDH_{\text{maximum release}} - LDH_{\text{natural release}})$$

2.11. Statistical analysis

Data were analyzed using GraphPad Prism software (version 7.0). Results are expressed as the mean ± standard deviation. A *t*-test was used to compare the two groups, and statistical significance was set at $P < 0.05$.

3. Results

3.1. Constructing recombinant plasmid and lentivirus packaging

The recombinant plasmid, denoted as pLV3-CMV-M2-T2A-FLUC-CopGFP, was constructed by *Eco*RI enzyme cleavage to excise the target fragment M2-T2A-FLUC from pCDNA3.1-M2-T2A-FLUC, followed by gel purification. The excised fragment was inserted into the pLV3-CMV-MCS-3 × FLAG-CopGFP-puromycin vector (Fig. 1A). Enzymatic cleavage identification and sequence analysis confirmed the structural and genetic composition of the expression plasmid, designated as pLV3-M2-FLUC. Fluorescence images at 24 h and 48 h post-Lent-M2 infection are presented in Fig. 1B. Flow cytometry was used to assess CopGFP expression under different lentiviral dilution gradients (Fig. 1C). The determined viral titer was 9.18 × 10^5 IU/mL.

3.2. Screening of the M2-FLUC-CopGFP stable cell line

YAC-1 cells were cultured with varying concentrations of puromycin for four days, with 80 % cell death observed in the wells at 2 μg/mL. Consequently, 2 μg/mL was determined as the optimal puromycin concentration for selective pressure screening. Lent-M2 was used to infect YAC-1 cells, and green fluorescence was observed under an inverted fluorescence microscope 48 h later, confirming the expression of CopGFP and indicating successful lentivirus infection. Following one week of continued cultivation under puromycin pressure, the cells were collected for FLUC expression analysis, which revealed the successful expression of firefly luciferase. Subsequently, single-cell clones with high CopGFP expression were isolated by flow cytometry (Fig. 2A), resulting in the acquisition of 70 individual clones. After screening under hygromycin pressure (2 μg/mL), four clones exhibiting elevated CopGFP expression were selected. Western blotting and qPCR analyses revealed that all four monoclonal cell lines showed detectable M2 expression (Fig. 2B, 2C). As clone 35 (C35) exhibited the highest relative expression of M2 mRNA and protein, it was selected for subsequent ADCC experiments. C35 cells were continuously passaged up to the 5th generation for western blotting, immunofluorescence, and flow cytometry analyses, demonstrating sustained and stable expression of M2 (Fig. 3A-C).

3.3. Isolation and identification of NK cells

Mouse splenocytes were isolated and ground through a 300-mesh stainless steel screen, followed by density gradient centrifugation for

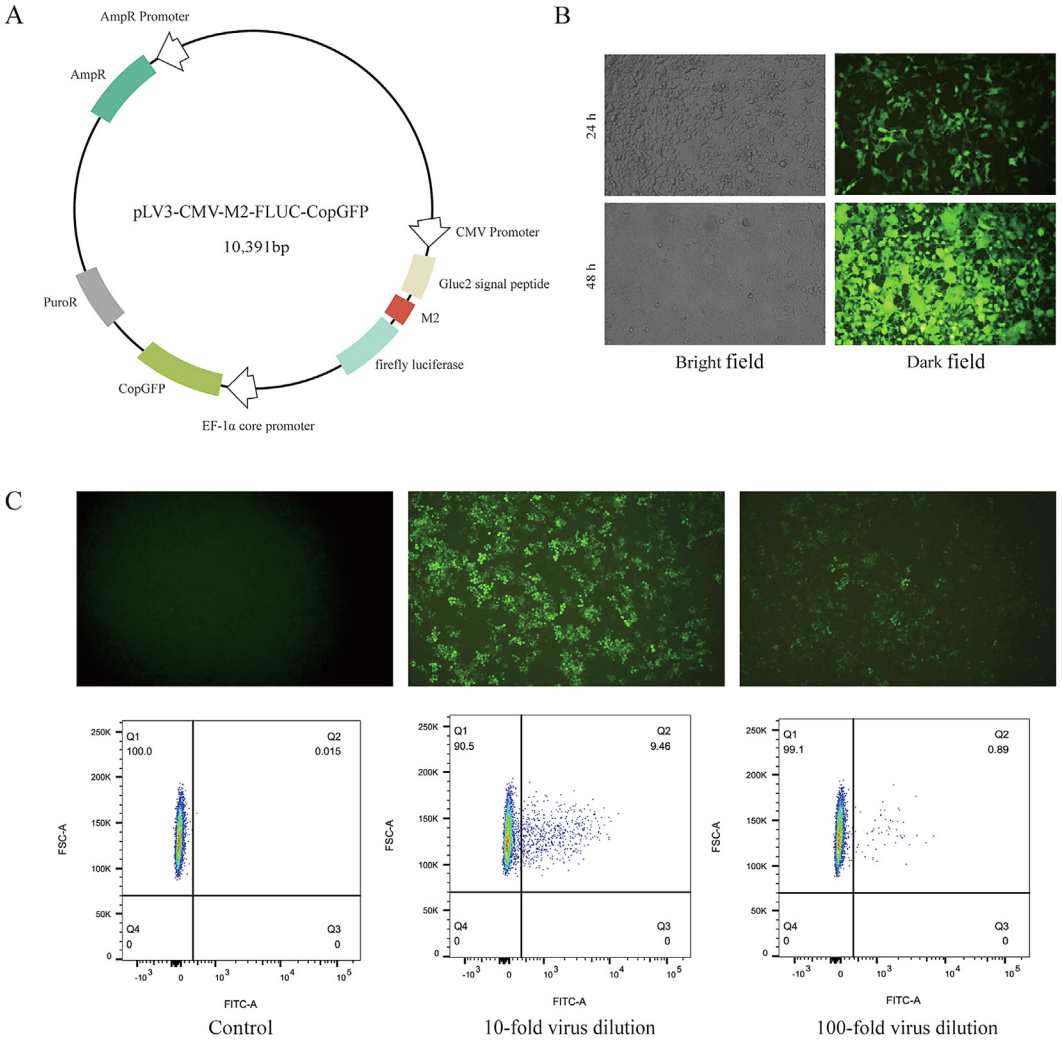

Fig. 1. Packaging and titration of lentivirus. A) Schematic of the lentivirus packaging plasmid containing M2. B) 24 h and 48 h fluorescence images showing lentivirus packaging. C) CopGFP expression in lentivirus-infected YAC-1 cells was detected under different dilution gradients. Abbreviations: M2, matrix protein 2; FITC-A, fluorescein isothiocyanate-area; FSC-A, forward scatter-area; CopGFP, Copepoda green fluorescent protein.

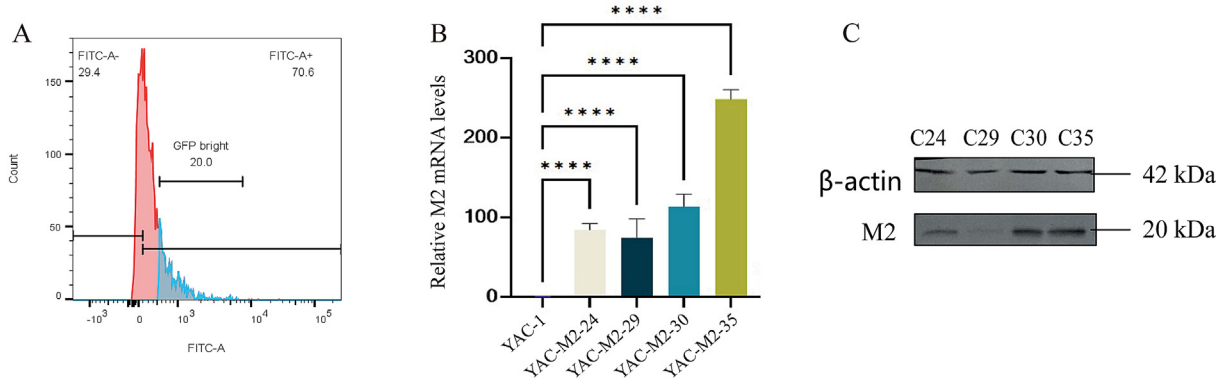

Fig. 2. Screening for M2-FLUC-CopGFP cells. A) Flow cytometry sorting of cells. B) Relative *M2* mRNA levels in monoclonal cell lines. Data are presented as mean ± standard deviation; *t*-test, **** $P < 0.001$ in comparison to the control YAC-1 cells. C) Western blot showing M2 expression in the four selected monoclonal cell lines. Abbreviations: M2, matrix protein 2; FITC, fluorescein isothiocyanate; CopGFP, Copepoda green fluorescent protein.

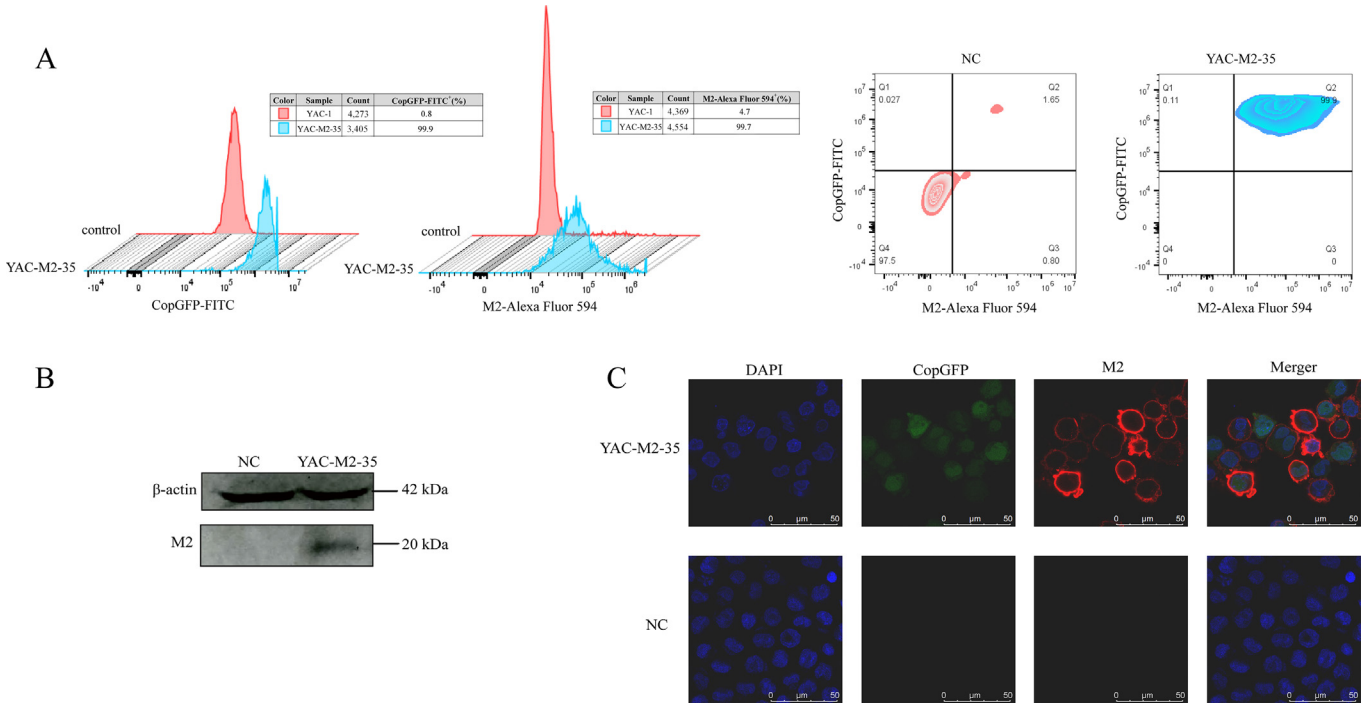

Fig. 3. M2 expression in monoclonal cell line C35. A) Flow cytometry indicating the expression of CopGFP and M2. B) and C) Stable expression of M2 in the 35th cell line detected by western blotting (B) and immunofluorescence (C). Abbreviations: M2, matrix protein 2; NC, negative control; FITC, fluorescein isothiocyanate; CopGFP, Copepoda green fluorescent protein.

initial screening. Subsequently, NK cells were isolated via negative selection using magnetic beads (Fig. 4A). Flow cytometry analysis revealed an increased purity of CD49b$^+$/CD3e$^-$ cells (NK cells) to 71.1 % (Fig. 4B).

3.4. Antibody detection and immunoprotective effect

A significant increase in M2e-specific antibodies ($P < 0.001$) was observed post-M2e immunization, with the titers escalating to 1×10^4 and 2.88×10^4 at 2 and 6 weeks post-immunization, respectively (Fig. 5A). Subtype analysis of antibodies IgG1 and IgG2a revealed that the M2e immunized group had a higher titer of M2e-specific IgG2a, with the IgG2a: IgG1 ratio significantly exceeding 1 (Fig. 5B). In the lethality test with 20 × LD_{50} PR8 influenza virus, the control group of mice began to show mortality starting from 3 days post-infection, with all mice decreasing by day 6. In contrast, mice immunized with LPP-4M2eNP exhibited their lowest body weight around 4 days post-infection, dropping to approximately 90 % of their initial weight (Fig. 5C). Subsequently, their body weight gradually recovered. The mice in this group experienced mortality between days 4 and 5 post-infection, with a survival rate of 50 % (Fig. 5D), indicating that immunization with LPP-4M2eNP conferred protection to mice against the virus.

3.5. Function identification of M2-FLUC-CopGFP stable transmissible cell line in vitro

The structural diagram of the influenza virus M2 [25] and a schematic representation of the ADCC effect can be found in Fig. 5E, 5F. The release of LDH in the cell culture supernatant was measured following co-incubation with YAC-1-M2 and M2e antibodies and NK cells. The M2e monoclonal antibody 14C2 exhibited marginal cytotoxicity, whereas the M2e immune mouse serum demonstrated a more

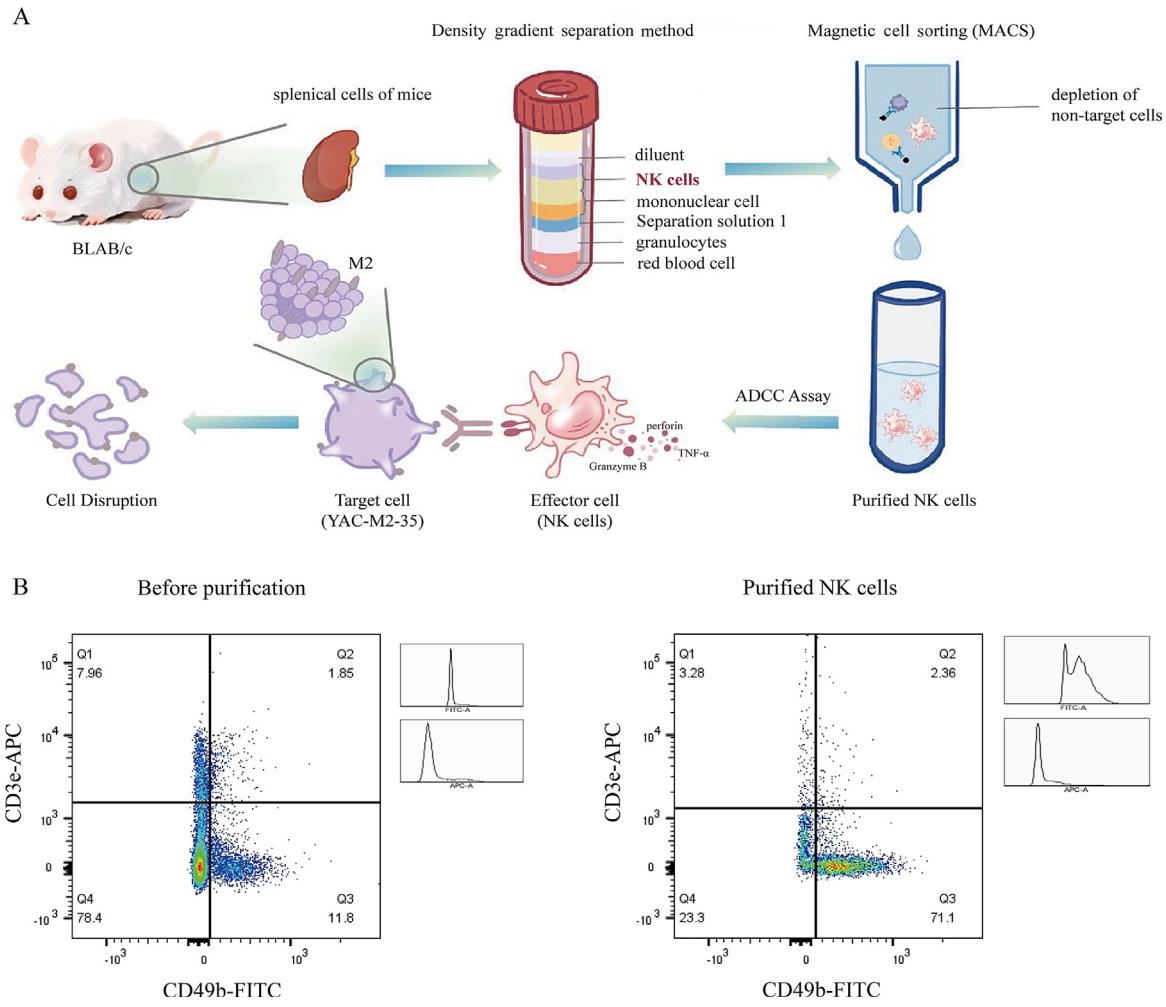

Fig. 4. NK cell isolation. A) Schematic illustrating the process of NK cell isolation. The final illustration in the panel shows the ADCC effect. B) Efficacy of NK cell isolation. Abbreviations: NK, natural killer; ADCC, antibody-dependent cell-mediated cytotoxicity; FITC, fluorescein isothiocyanate; APC, Allophycocyanin .

pronounced cytotoxic effect. Cytotoxic efficacy displayed a dose-dependent relationship with antibody dilution. Additionally, an increase in the effector-to-target ratio was associated with increased cytotoxic efficiency. The results in Fig. 5H demonstrate that an effector-to-target ratio of 20:1 provides a more robust response in ADCC efficacy. Therefore, subsequent experiments adopted a 20:1 effector-to-target ratio to evaluate the ADCC efficacy using various serum dilutions, as depicted in Fig. 5G.

4. Discussion

The protective role of influenza virus M2 through ADCC has been demonstrated [26]. Establishing a reliable method for detecting ADCC involving M2 is crucial to elucidate the protective mechanisms associated with M2. However, there is limited data available on the accurate assessment of the efficacy of M2. The commonly employed target cells in previous ADCC assessments of influenza viruses were MDCK cells infected with the influenza virus. However, the surface expression of M2 in such infected cells is relatively low [27], rendering them less suitable for use as target cells. Plasmids containing influenza virus-specific genes have also been transiently transfected into target cells [28]. However, transient transfection of target cells for each experiment leads to poor stability and consistency, which may affect the accuracy of the detection results. In this study, a stable cell line expressing the M2 protein of the IAV (termed YAC-1-M2) was established by infecting YAC-1 cells with a lentivirus. The YAC-1-M2 cell line exhibited high and enduring M2 expression, enabling convenient and long-term experimental investigations.

Currently, the Jurkat-Lucia NFAT-CD16 cell line is frequently used as effector cells for assessing the effects of ADCC. This cell line expresses the CD16 (FCγRIII) receptor (IgG Fc receptor). The binding of the target, antibody, and receptor activates the Nuclear Factor of Activated T-cells (NFAT), driving the expression of luciferase. This system provides a means of artificially establishing T cells expressing FcRs [29,30]. However, there may be functional differences between artificially engineered T cells expressing FcRs and NK cells that inherently express FcRs. Moreover, this cell line is relatively expensive, restricting its widespread adoption in typical laboratories. In this study, activated mouse NK cells were used as effector cells owing to their comparatively low cost and excellent reproducibility, facilitating broader applicability in standard laboratory settings. This study directly assessed cytotoxicity by measuring LDH release from target cells, providing an immediate and accurate reflection of cytotoxic efficacy. This method is theoretically superior to relying on indirect indicators, such as effector cell activation. Of the various types and subtypes of antibodies (including IgA, IgM, and IgG) that induce ADCC, IgG is the predominant ADCC mediator. In murine models, ADCC activity is primarily facilitated by the interaction between mouse IgG2a and mouse FcγRIV [31].

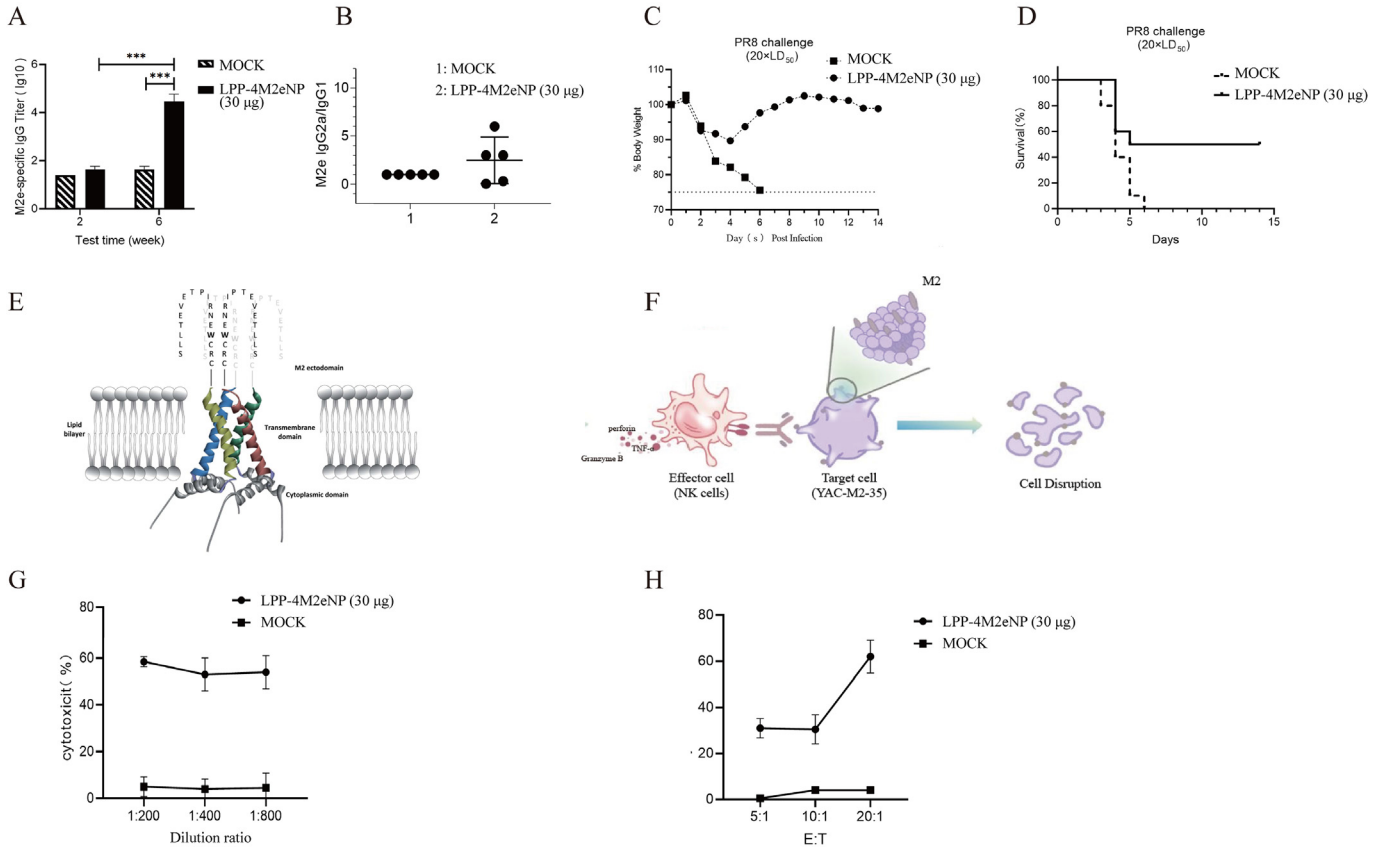

Fig. 5. Vaccine evaluation and antibody-dependent cell-mediated cytotoxicity. A) Detection of specific IgG induced by LPP-4M2eNP immunization. B) IgG1 and IgG2a subtypes induced by LPP-4M2eNP immunization. C) Survival of LPP-4M2eNP-immunized BALB/c mice challenged with 20 × LD_{50} of influenza A virus PR8. D) Monitoring of body weight in mice after PR8 challenge. E) M2 structure. F) Illustration of antibody-dependent cell-mediated cytotoxicity assay. G) Cytotoxicity at effector-target ratio of 20:1. H) Antibody-mediated killing rate of NK cells under different antibody dilution and target ratios. Abbreviations: NK, natural killer; M2, matrix protein; LPP, lipopolyplex; MOCK, mock control; LD, lethal dose; E:T, effector-to-target ratio.

In this study, the *M2* mRNA vaccine demonstrated effective immune protection against influenza virus attacks in mice, as evidenced by robust immune protection (unpublished results). The findings of this study indicate that mice sera exhibit ADCC effects induced by M2e-based immunization, suggesting a potential mechanism through which the vaccine confers immune protection. Furthermore, the use of the M2 monoclonal antibody 14C2 revealed a diminished cytotoxic effect, implying a potential association with the antibody subtypes.

Previous research findings suggest a correlation between the antibody-binding affinity and the mFcγRIV-mediated ADCC in mice [32,33]. The hierarchy of ADCC efficacy among the IgG subclasses is IgG2a > IgG2b > IgG1. The 14C2 antibody belongs to the IgG1 subtype. Notably, the *M2* mRNA vaccine-induced antibodies comprised both the IgG2a and IgG1 subtypes, with the IgG2a: IgG1 ratio significantly exceeding 1. Consequently, antibodies induced by the *M2* mRNA vaccine exhibited enhanced ADCC efficacy compared with the M2 monoclonal antibody, which demonstrated only marginal ADCC effects. This observation aligns with previous research. In conclusion, we successfully established a stable cell line (YAC-1-M2) sustaining M2 expression. This cell line is a valuable tool to investigate the immunoprotective mechanisms associated with influenza virus M2 protein and can help enhance our understanding of the mechanisms underlying ADCC in the context of influenza M2. Additionally, this approach may apply to the study of other antigens or pathogenic agents.

In summary, we here developed a novel method to assess ADCC associated with M2-based immunization in mice, which paves the way for the development of an M2-based universal vaccine against IAV and an in-depth analysis of its mechanism of broad-spectrum immune protection in mice.

Ethics statement

Our animal experiments were conducted at the Animal Center of Beijing Kexing Vaccine Co., Ltd., in accordance with the guidelines of the Institutional Laboratory Animal Care and Use Committee (No. 20210315025).

Acknowledgements

This work was supported by the National Key Research and Development Program of China (2021YFC2300101).

Conflict of interest statement

The authors declare that there are no conflicts of interest.

Author contributions

Yinjie Liang: Data curation, Writing – original draft. **Junjia Guo:** Data curation, Writing – original draft. **Zhen Li:** Data curation, Writing – original draft. **Shiyuan Liu:** Investigation, Writing – review & editing. **Ting Zhang:** Data curation, Writing – original draft. **Shucai Sun:** Data curation, Writing – original draft. **Funa Lu:** Investigation, Writing – review & editing. **Yuqian Zhai:** Investigation, Writing –

review & editing. **Wenling Wang:** Conceptualization, Methodology, Writing – review & editing. **Chuanyi Ning:** Conceptualization, Methodology, Writing – review & editing. **Wenjie Tan:** Conceptualization, Methodology, Writing – review & editing.

References

[1] R.J. Sugrue, A.J. Hay, Structural characteristics of the M2 protein of influenza A viruses: evidence that it forms a tetrameric channel, Virology 180 (1991) 617–624, https://doi.org/10.1016/0042-6822(91)90075-m.

[2] S. Li, C. Sieben, K. Ludwig, C.T. Höfer, S. Chiantia, A. Herrmann, F. Eghiaian, I.A. Schaap, pH-Controlled two-step uncoating of influenza virus, Biophys. J. 106 (2014) 1447–1456, https://doi.org/10.1016/j.bpj.2014.02.018.

[3] K. Das, J.M. Aramini, L.C. Ma, R.M. Krug, E. Arnold, Structures of influenza A proteins and insights into antiviral drug targets, Nat. Struct. Mol. Biol. 17 (2010) 530–538, https://doi.org/10.1038/nsmb.1779.

[4] S.M. Ebrahimi, M. Tebianian, Influenza A viruses: why focusing on M2e-based universal vaccines, Virus Genes 42 (2011) 1–8, https://doi.org/10.1007/s11262-010-0547-7.

[5] T.M. Fu, D.C. Freed, M.S. Horton, J. Fan, M.P. Citron, J.G. Joyce, V.M. Garsky, D.R. Casimiro, Q. Zhao, J.W. Shiver, X. Liang, Characterizations of four monoclonal antibodies against M2 protein ectodomain of influenza A virus, Virology 385 (2009) 218–226, https://doi.org/10.1016/j.virol.2008.11.035.

[6] U. Kumar, P. Goyal, Z.K. Madni, K. Kamble, V. Gaur, M.S. Rajala, D.M. Salunke, A structure and knowledge-based combinatorial approach to engineering universal scFv antibodies against influenza M2 protein, J. Biomed. Sci. 30 (2023) 56, https://doi.org/10.1186/s12929-023-00950-2.

[7] L.D. Nesovic, C.J. Roach, G. Joshi, H.S. Gill, Delivery of gold nanoparticle-conjugated M2e influenza vaccine in mice using coated microneedles, Biomater. Sci. 11 (2023) 5859–5871, https://doi.org/10.1039/d3bm00305a.

[8] M.J. Ouyang, Z. Ao, T.A. Olukitibi, P. Lawrynuik, C. Shieh, S.K.P. Kung, K.R. Fowke, D. Kobasa, X. Yao, Oral immunization with rVSV bivalent vaccine elicits protective immune responses, including ADCC, against both SARS-CoV-2 and influenza A viruses, Vaccines (Basel) 11 (2023) 1404, https://doi.org/10.3390/vaccines11091404.

[9] A.A. Zykova, E.A. Blokhina, L.A. Stepanova, M.A. Shuklina, O.O. Ozhereleva, L.M. Tsybalova, V.V. Kuprianov, N.V. Ravin, Nanoparticles carrying conserved regions of influenza A hemagglutinin, nucleoprotein, and M2 protein elicit a strong humoral and T cell immune response and protect animals from infection, Molecules 28 (2023) 6441, https://doi.org/10.3390/molecules28186441.

[10] V.R. Simhadri, M. Dimitrova, J.L. Mariano, O. Zenarruzabeitia, W. Zhong, T. Ozawa, A. Muraguchi, H. Kishi, M.C. Eichelberger, F. Borrego, A human anti-M2 antibody mediates antibody-dependent cell-mediated cytotoxicity (ADCC) and cytokine secretion by resting and cytokine-preactivated natural killer (NK) cells, PLoS One 10 (2015) e0124677, https://doi.org/10.1371/journal.pone.0124677.

[11] J.M. Reichert, Antibody Fc: Linking Adaptive and Innate Immunity, mAbs 6 (2014) 619–621, https://doi.org/10.4161/mabs.28617.

[12] T. Timonen, E. Saksela, A simplified isotope release assay for cell-mediated cytotoxicity against anchorage dependent target cells, J. Immunol. Methods. 18 (1977) 123–132, https://doi.org/10.1016/0022-1759(77)90163-6.

[13] A.E. Lee-MacAry, E.L. Ross, D. Davies, R. Laylor, J. Honeychurch, M.J. Glennie, D. Snary, R.W. Wilkinson, Development of a novel flow cytometric cell-mediated cytotoxicity assay using the fluorophores PKH-26 and TO-PRO-3 iodide, J. Immunol. Methods 252 (2001) 83–92, https://doi.org/10.1016/s0022-1759(01)00336-2.

[14] D.B. Jacobs, C. Pipho, Use of propidium iodide staining and flow cytometry to measure anti-mediated cytotoxicity: resolution of complement-sensitive and resistant target cells, J. Immunol. Methods 62 (1983) 101–108, https://doi.org/10.1016/0022-1759(83)90115-1.

[15] V.R. Gómez-Román, R.H. Florese, L.J. Patterson, B. Peng, D. Venzon, K. Aldrich, M. Robert-Guroff, A simplified method for the rapid fluorometric assessment of antibody-dependent cell-mediated cytotoxicity, J. Immunol. Methods 308 (2006) 53–67, https://doi.org/10.1016/j.jim.2005.09.018.

[16] M. Broussas, L. Broyer, L. Goetsch, Evaluation of antibody-dependent cell cytotoxicity using lactate dehydrogenase (LDH) measurement, Methods Mol. Biol. 988 (2013) 305–317, https://doi.org/10.1007/978-1-62703-327-5_19.

[17] K. Kato, T. Agatsuma, T. Tanabe, T. Masuko, Y. Hashimoto, Release of esterase from murine lymphokine-activated killer cells in antibody-dependent cellular cytotoxic reaction, Jpn. J. Cancer Res. 82 (1991) 206–212, https://doi.org/10.1111/j.1349-7006.1991.tb01830.x.

[18] J.R. Ortaldo, R.T. Winkler-Pickett, K. Nagashima, H. Yagita, K. Okumura, Direct evidence for release of pore-forming protein during NK cellular lysis, J. Leukoc. Biol. 52 (1992) 483–488, https://doi.org/10.1002/jlb.52.5.483.

[19] A.W. Chung, E. Rollman, R.J. Center, S.J. Kent, I. Stratov, Rapid degranulation of NK cells following activation by HIV-specific antibodies, J. Immunol. 182 (2009) 1202–1210, https://doi.org/10.4049/jimmunol.182.2.1202.

[20] W. Wang, B. Huang, Y. Deng, X. Wang, W. Tan, L. Ruan, Expression of influenza A3 virus (H3N2) M2 gene in vaccinia virus Tiantan strain, Chin. J. Virol. 23 (2007) 377–383, https://doi.org/10.3321/j.issn:1000-8721.2007.05.008.

[21] Q. Song, W. Wang, Y. Zhan, F. Lu, Y. Deng, W. Tan, Optimization of signal peptide sequences of spike protein subunit of MERS-CoV for secretory expression in eukaryotic cells, Chin. J. Virol. 35 (2019) 20–26, https://doi.org/10.13242/j.cnki.bingduxuebao.003487.

[22] L. Mekkaoui, E.M. Bentley, M. Ferrari, K. Lamb, K. Ward, J. Sillibourne, S. Onuoha, G. Mattiuzzo, Y. Takeuchi, M. Pule, et al., Optimised method for the production and titration of lentiviral vectors pseudotyped with the SARS-CoV-2 spike, Bio Protoc. 11 (2021) e4194, https://doi.org/10.21769/BioProtoc.4194.

[23] J. Guo, W. Wang, Y. Deng, B. Huang, F. Ye, A. Ruhan, N. Wang, X. Sun, W. Tan, Immune responses elicited by influenza A mRNA vaccine based on lipopolyplex-encapsulated virus nucleoprotein and matrix protein 2 extracellular domain fusion in mice, Chin. J. Microbiol. Immunol. 3 (2022) 209–215, https://doi.org/10.3760/cma.j.cn112309-20220107-00007.

[24] T. Oyamada, S. Okano, Cytotoxicity effect of trastuzumab on canine peripheral blood mononuclear cells, Iran. J. Vet. Res. 21 (2020) 263–268, https://doi.org/10.22099/IJVR.2020.38112.5553.

[25] F. Kostolanský, K. Tomčíková, K. Briestenská, et al., Universal anti-influenza vaccines based on viral HA2 and M2e antigens, Acta. Virol. 64 (4) (2020) 417–426, https://doi.org/10.4149/av_2020_408.

[26] M. De Filette, A. Ramne, A. Birkett, N. Lycke, B. Löwenadler, W. Min Jou, X. Saelens, W. Fiers, The universal influenza vaccine M2e-HBc administered intranasally in combination with the adjuvant CTA1-DD provides complete protection, Vaccine 24 (2006) 544–551, https://doi.org/10.1016/j.vaccine.2005.08.061.

[27] V. Chromikova, J. Tan, S. Aslam, A. Rajabhathor, M. Bermudez-Gonzalez, J. Ayllon, V. Simon, A. García-Sastre, B. Salaun, R. Nachbagauer, et al., Activity of human serum antibodies in an influenza virus hemagglutinin stalk-based ADCC reporter assay correlates with activity in a CD107a degranulation assay, Vaccine 38 (2020) 1953–1961, https://doi.org/10.1016/j.vaccine.2020.01.008.

[28] L. Shi, Y. Long, Y. Zhu, J. Dong, Y. Chen, H. Feng, X. Sun, VLPs containing stalk domain and ectodomain of matrix protein 2 of influenza induce protection in mice, Virol. J. 20 (2023) 38, https://doi.org/10.1186/s12985-023-01994-4.

[29] R.G.E. Krause, T. Moyo-Gwete, S.I. Richardson, Z. Makhado, N.P. Manamela, T. Hermanus, N.N. Mkhize, R. Keeton, N. Benede, M. Mennen, et al., Infection pre-Ad26.COV2.S-vaccination primes greater class switching and reduced CXCR5 expression by SARS-CoV-2-specific memory B cells, Npj Vaccines 8 (2023) 119, https://doi.org/10.1038/s41541-023-00724-9.

[30] K.A. Giang, T. Boxaspen, Y. Diao, J. Nilvebrant, M. Kosugi-Kanaya, M. Kanaya, S.Z. Krokeide, F. Lehmann, S. Svensson Gelius, K.J. Malmberg, et al., Affibody-based hBCMA x CD16 dual engagers for NK cell-mediated killing of multiple myeloma cells, N, Biotechnol. 77 (2023) 139–148, https://doi.org/10.1016/j.nbt.2023.09.002.

[31] D.M. Carragher, D.A. Kaminski, A. Moquin, L. Hartson, T.D. Randall, A novel role for non-neutralizing antibodies against nucleoprotein in facilitating resistance to influenza virus, J. Immunol. 181 (2008) 4168–4176, https://doi.org/10.4049/jimmunol.181.6.4168.

[32] M. Guilliams, P. Bruhns, Y. Saeys, H. Hammad, B.N. Lambrecht, The function of Fcγ receptors in dendritic cells and macrophages, Nat. Rev. Immunol. 14 (2014) 94–108, https://doi.org/10.1038/nri3582.

[33] F. Nimmerjahn, J.V. Ravetch, Fcgamma receptors: old friends and new family members, Immunity 24 (2006) 19–28, https://doi.org/10.1016/j.immuni.2005.11.010.